Observations of a Radial Density Gradient in the Very Local Interstellar Medium by Voyager 2

W. S. Kurth and D. A. Gurnett
Department of Physics and Astronomy, University of Iowa, Iowa City, IA 52242, USA; william-kurth@uiowa.edu
Received 2020 July 29; accepted 2020 August 12; published 2020 August 25

Abstract

Beginning on 2020 June 19, at a heliocentric distance of 124.2 au, the Voyager 2 Plasma Wave Science instrument began to observe radio emissions followed by electron plasma oscillations in its 3.11 kHz spectrum analyzer channel. Plasma oscillations at this frequency imply an electron density in the range of $0.12\,\mathrm{cm}^{-3} \pm 15\%$, although some response in the 1.78 kHz channel near the peak of the plasma oscillations suggest a density of $0.087\,\mathrm{cm}^{-3} \pm 8\%$. Shortly after Voyager 2 crossed the heliopause, in late 2019 January, the Voyager 2 Plasma Wave Science instrument detected plasma oscillations in its 1.78 kHz channel giving an electron density of $0.039\,\mathrm{cm}^{-3} \pm 15\%$. While the Voyager spectrum analyzer affords relatively poor spectral resolution, the recent observation of plasma oscillations in the 3.11 kHz channel provides definitive evidence of a radial density gradient in the very local interstellar medium (VLISM), just beyond the heliopause with a magnitude similar to that observed by Voyager 1 obtained with higher spectral resolution measurements. Plasma oscillations observed by Voyager 1 range from frequencies as low as 2.1 kHz increasing to about 3.2 kHz, giving an electron density profile that increases from about 0.055 to about $0.13\,\mathrm{cm}^{-3}$ over a distance spanning some 20 au. Given the 67° difference in heliographic latitude and 43° difference in longitude between the two Voyagers, the new Voyager 2 observations imply that the density gradient is a large-scale feature of the VLISM in the general direction of the heliospheric nose.

Unified Astronomy Thesaurus concepts: Interstellar medium (847); Interstellar plasma (851)

1. Introduction

Voyager 1 crossed the heliopause into the very local interstellar medium (VLISM) on 2012 August 25 at a heliocentric radial distance of 121.6 au (Burlaga et al. 2013; Gurnett et al. 2013; Krimigis et al. 2013; Stone et al. 2013). While the Voyager 1 Plasma Science (PLS) instrument was not operational, the Plasma Wave Science (PWS) instrument has observed electron plasma oscillations on a number of occasions through 2019 and distances up to about 145 au (Gurnett et al. 2013, 2015; Pogorelov et al. 2017; Gurnett & Kurth 2019). The frequencies of the observed emissions ranged from 2.1 to 3.2 kHz rising in a near monotone fashion. As the electron plasma frequency f_{pe} is $8980(n_e)^{1/2}$, where frequency is in Hz and the electron density n_e is in cm^{-3}, the observations show a radial density gradient increasing from 0.055 to $0.13\,\mathrm{cm}^{-3}$.

Voyager 2 crossed the heliopause on 2018 November 5 at a distance of 119.0 au (Burlaga et al. 2019; Krimigis et al. 2019; Richardson et al. 2019; Stone et al. 2019). Because of the relatively cold plasma temperature and the direction of the inflowing plasma, the Voyager 2 PLS instrument could not provide well-constrained moments of the plasma distribution function. However, at the end of 2019 January the Voyager 2 PWS instrument detected a plasma oscillation event in its 1.78 kHz spectrum analyzer channel, yielding an electron plasma density of $0.039\,\mathrm{cm}^{-3} \pm 15\%$ at a distance 119.7 au (Gurnett & Kurth 2019).

In this Letter we discuss the detection of a new electron plasma oscillation event by the Voyager 2 PWS at a distance of 124.2 au in the 3.11 kHz channel of the instrument. This detection provides evidence of an increase in density from that observed at 119.7 au, hence the existence of a radial density gradient similar to that observed by Voyager 1, and shows that this gradient is a large-scale feature of the heliopause-interstellar medium interaction in the direction of the heliospheric nose.

2. Observations

The new observations presented herein are from the Voyager 2 PWS instrument (Scarf & Gurnett 1977). The two Voyager instruments are identical in design and construction, utilizing two 10 m elements extended orthogonally as a balanced dipole antenna with an effective length of 7.07 m. Each instrument includes a 16-channel spectrum analyzer with center frequencies ranging from 10 Hz to 56.2 kHz. The upper eight channels used in this Letter have bandwidths of about ±7.5% and are spaced logarithmically with four channels per decade. For much of the mission beyond the planetary phase, each of these channels is sampled once per four seconds and the sums of these four measurements are telemetered to the ground, allowing for an ~16 s average for each channel. These measurements are made continuously, but are only received on the ground during tracking passes by the Deep Space Network.

Each instrument also has a wideband waveform channel with a bandpass of ~10 Hz to 12 kHz. The voltage detected by the preamplifier at the base of the antenna is sampled $28,800\,\mathrm{s}^{-1}$ and converted to a digital value with 4-bit accuracy. Using typical Fourier analysis parameters, the spectral resolution of these measurements is 28 Hz, which is superior to the spectrum analyzer. However, due to the high telemetry rate required for the wideband measurements (recorded at 115 kbps) these are used at very low duty cycles, about 48 s one to three times per week at Voyager's current distance.

Two issues on Voyager 2 have affected the PWS data. First, only a few months after launch, a failure occurred in the spacecraft data system involving a multiplexor, called a tree switch, that services the eight higher frequency spectrum
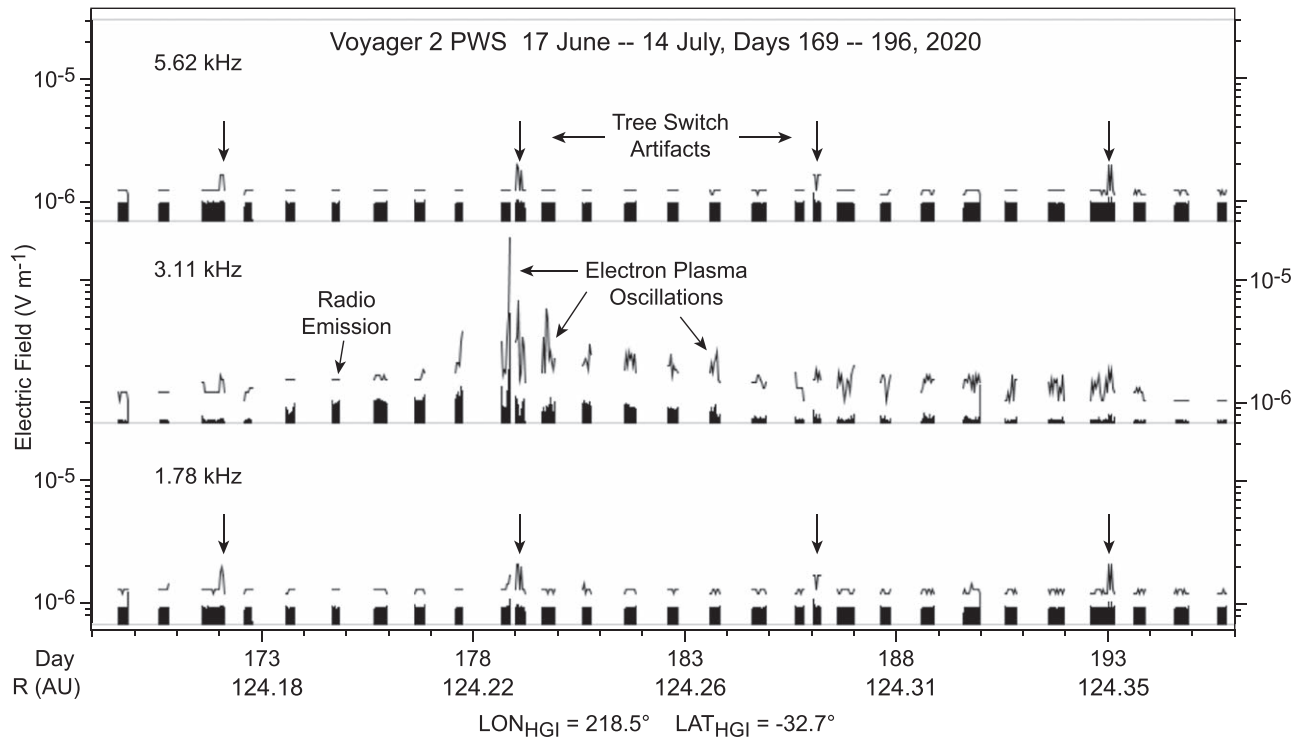
Figure 1. Electric field strength as a function for time for three Voyager 2 spectrum analyzer channels centered at 5.62, 3.11, and 1.78 kHz for the interval from days 169 to 196 2020. The height of the solid black areas at the bottom of each channel correspond to ∼51 minute averages, while the line above shows the peaks during the averaging intervals. The features marked with vertical arrows near the beginning of days 172, 179, 186, and 193 are artifacts related to an early-mission anomaly in the Voyager 2 spacecraft data system. The 3.11 kHz channel shows activity beginning on day 172 and ending on 193 related to electron plasma oscillations, although the smoothly varying activity from day173 to 176 is likely due to radio emissions propagating from a source where there are strong electron plasma oscillations.

analyzer channels (1.0–56.2 kHz) among other spacecraft parameters. This failure required an inflight recalibration for those eight channels that was successful and allowed ground-breaking observations at the four gas giants in the planetary phase of the Voyager mission, albeit with somewhat lower sensitivity. An additional aspect of the multiplexor issue is that the PWS data are prone to variations depending on other measurements that use the tree switch; these tend to be either rigidly periodic and timed by the spacecraft clock, or are quasi-periodic and depend on other activities on the spacecraft. These artifacts can usually be recognized and separated from natural signals.

The second issue involving the Voyager 2 PWS instrument was a gradual degradation of the wideband receiver channel to the point where no useful data were being produced. This portion of the Voyager 2 instrument was turned off in 2006. The effect of this is that the spectral resolution (and therefore the precision of electron density determinations) is generally limited to the spectrum analyzer resolution. However, in this Letter we take advantage of a special condition to improve on this for the recent event.

Figure 1 shows the amplitudes of signals in the Voyager 2 spectrum analyzer channels centered at 5.62, 3.11, and 1.78 kHz for the interval June 17 to July 14 (days 169–196) of 2020. For each channel the averages over ∼51 minute intervals are plotted as the height of the solid black area near the bottom of each panel. The peak measurements for the same ∼51 minute intervals are plotted above this connected by a line. The signal levels in the 3.11 kHz channel during the first two and last two days in the plotted interval represent the background level for this channel. Notice that near the beginning of the data from day 171 there is an increase in

this level in both the average and the peak. This constitutes the beginning of radio and plasma wave signals that last until early on day 193. The spike near the beginning of day 172 is an artifact from the above-described multiplexor issue and is identified by arrows in the 1.78 and 5.62 kHz channels at the same time. This artifact occurs approximately weekly during this time period and is also marked near the beginning of days 179, 186, and 193. We use the fact that this artifact occurs in multiple channels (in fact, all of the upper eight channels) as a solid indicator that this is an artifact and not a natural signal. The activity in the 3.11 kHz channel is last observed during day 193, primarily in the peak amplitude. On days 173 through 175, there is little fluctuation in the peak values. Much of the variation in the average values for these days may be attributed to an increasing signal level with time. We interpret these emissions as radio waves generated by mode conversion of electron plasma oscillations remote from Voyager. A similar effect was observed on Voyager 1, particularly during the 2014 event described by Gurnett et al. (2015).

Beginning on or about day 176, the level of fluctuations and the intensity of the signal in the 3.11 kHz channel increase to a peak late on day 178. Fluctuations are observed especially in the peaks until near the end of the event on day 193. There is a definite decrease in amplitude in both the peaks and averages occurring between day 183 and 184. This, too, is reminiscent of the Voyager 1 2014 event and may signal the passage of a shock, although we cannot determine this without complimentary observations, for example, from the magnetometer.

Figure 2 shows an expanded time interval from late on day 178, from 20:30 to 21:25 UT. For this expanded plot, the temporal resolution is such that each 16 s average can be plotted. Note that the periodic gaps occur because of the
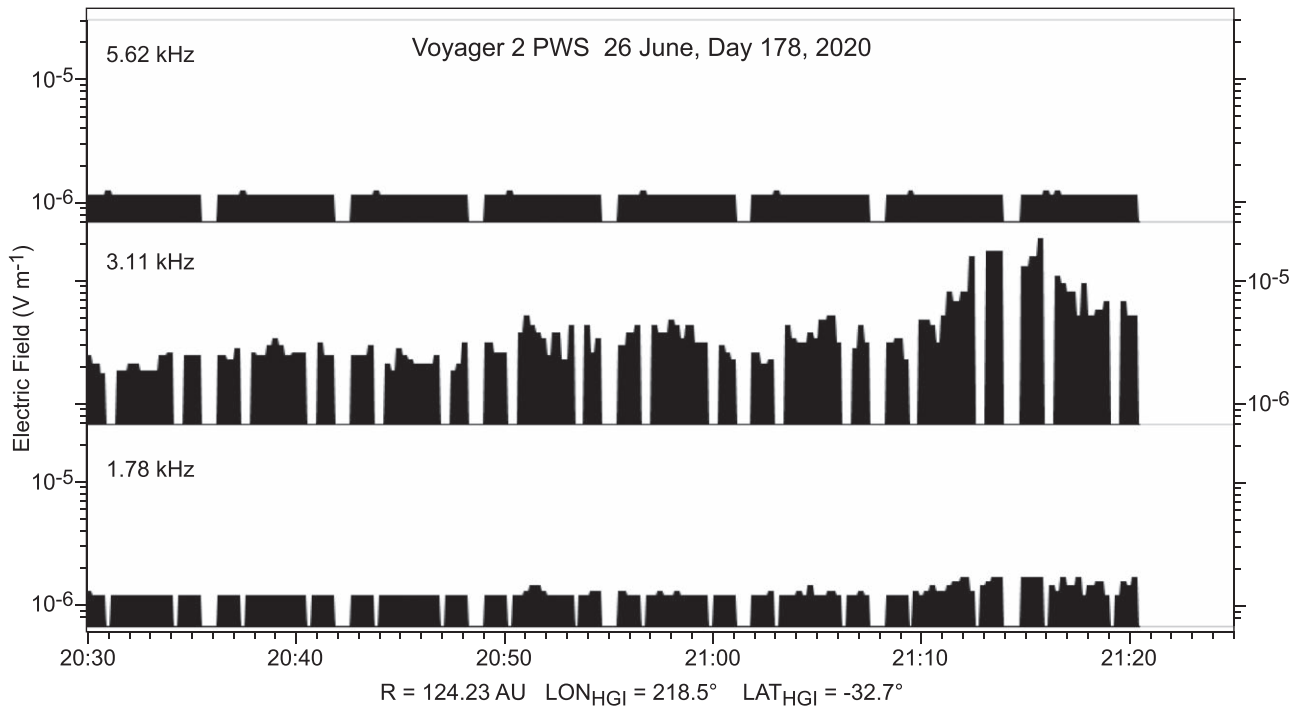
Figure 2. An expanded time interval from Figure 1 in a similar format. Here, the temporal resolution is such that each 16 s average telemetered from the spacecraft is visible. The gaps are due to known multiplexor artifacts being omitted. Note that near the peak of emissions centered near 21:15 on day 178 there is also a response in the 1.78 kHz channel.

removal of periodic tree switch artifacts that are linked to the spacecraft clock. This timing characteristic is an additional way in which the multiplexor artifacts can be identified and, in this case, eliminated from the plot. The primary purpose of this expanded plot is to point out that there is a clear response in the 1.78 kHz channel when the 3.11 kHz signal increases. This is particularly apparent around 21:15 at the peak of the event. At this time, the maximum electric field in the 3.11 kHz channel is $2.19 \times 10^{-5} \, \mathrm{V} \, \mathrm{m}^{-1}$. The corresponding amplitude at 1.78 kHz is $1.71 \times 10^{-6} \, \mathrm{V} \, \mathrm{m}^{-1}$. We note that there is basically no response in the 5.62 kHz channel, which has a baseline amplitude of $1.12 \times 10^{-6} \, \mathrm{V} \, \mathrm{m}^{-1}$.

In the Supplementary Information supplied with Gurnett & Kurth (2019), the measured ratio of signal strengths observed in channels adjacent to the 1.78 kHz channel are used to narrow the possible frequency of the signal in that channel. In this case, there was no visible response in either the 1.00 or 3.11 kHz channels, so Gurnett & Kurth (2019) used the ratio of the 1.78 emission to the background levels of the adjoining channels as the lower limit of relative signal strengths. As shown in their Figure S1, this bounded the possible frequency of the emission in the 1.78 kHz channel to about $\pm 7.5\%$ of the center frequency, leading to upper and lower bounds of 1.895 and 1.658 kHz, respectively. The corresponding range of n_e based on this analysis was 0.0454–$0.0347 \, \mathrm{cm}^{-3}$.

For the event reported here, a special condition is observed for a short interval on day 178. That is, we measure the intensity of the emission in two adjacent channels of the spectrum analyzer. If we assume a narrowband emission, as is typical for electron plasma oscillations, we can estimate the frequency by measuring the ratio of the signal strength in the two channels, and use the frequency responses of the two channels to determine which frequency gives the observed intensity ratio. We use measured filter responses of the 1.78,
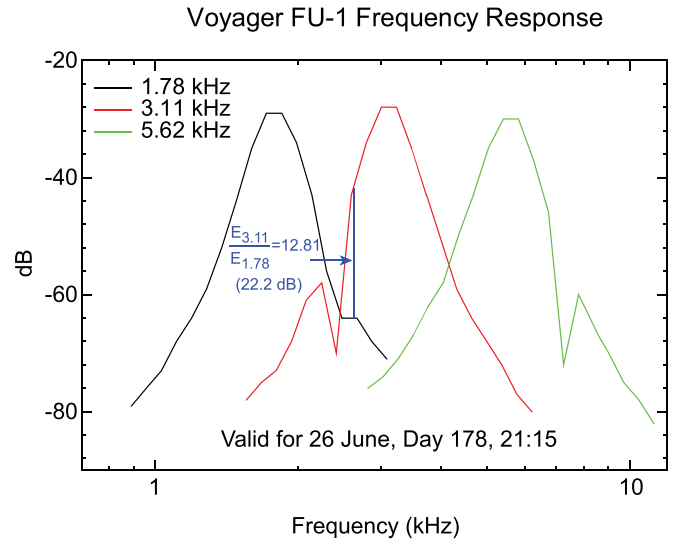

Figure 3. Frequency response curves from the identical Voyager 1 instrument for the 1.78, 3.11, and 5.62 kHz channels. The blue line segment near 2.65 kHz has a height of 22.2 dB, and the ratio of the electric field strengths at 21:15 on day 178 when a response is seen both in the 3.11 and 1.78 kHz channels with a 22.2 dB ratio. Such a ratio is allowed by the filter responses only very close to 2.65 kHz and provides the basis for determining the electron density near $0.087 \, \mathrm{cm}^{-3}$.

3.11, and 5.62 kHz filters recovered for the FU-1 instrument, which flew on Voyager 1. Similar data have not been found for the Voyager 2 instrument, but the filters used for the upper eight channels of the Voyager spectrum analyzers were procured to identical specifications. Therefore, we believe that the FU-1 frequency response is a valid one to use for Voyager 2, in the absence of other data. We have reproduced the frequency response curves in Figure 3. It should be noted that because the Voyager spacecraft used an AC power supply at a

frequency of 2.4 kHz, the PWS instrument had notch filters at 2.4 and 7.2 kHz to minimize interference from the power supply fundamental frequency and third harmonic. The filter responses in Figure 3 include the effect of these filters. We note that this particular test data used 7% frequency steps, hence the resolution of the responses is correspondingly limited.

We compute the ratio of the electric field strength measured in the 3.11 kHz channel and the 1.78 kHz channel: $2.19 \times 10^{-5}/1.71 \times 10^{-6} = 12.81$ or 22.2 dB. Next, we locate a position in Figure 3 where the ratio of the filter responses for 3.11 and 1.78 kHz is 22.2 dB using a dark blue line. While this is close to the 2.4 kHz notch filter that is not fully resolved in the response curves, it is clear that the signal would have to be very close to 2.65 kHz to exhibit the observed ratio. Given the measured ratio of the peak signal in the 3.11 and 1.78 kHz channels, it is difficult to argue that the frequency of the emission is much different than 2.65 kHz. The slopes in the filter responses are quite steep, especially near the notch filter. Consequently, even given the 7% spectral resolution in the filter responses, the frequency at which the observed 22.2 dB ratio matches the difference in the filter responses cannot deviate more than about 100 Hz from the frequency shown in Figure 3. We estimate that the uncertainty in the frequency leading to the observed ratio of electric fields is about ±100 Hz, giving a range of electron densities of 0.081–0.094 cm^{-3}. We conclude that n_e is 0.087 cm^{-3} ± 8% at $R = 124.2$ au for the short interval on day 178 where the plasma oscillations peak in amplitude and are observed in both the 1.78 and 3.11 kHz channels.

We should also say that the recalibration of the upper eight spectrum analyzer channels due to the tree switch failure may be considered another source of uncertainty, if this means that the relative amplitude of the response in adjacent channels is not well known. However, the recalibration algorithm based on Voyager Project analysis of this failure was uniformly applied to all of the upper eight channels of the spectrum analyzer. This means that while the absolute intensity of the detected plasma oscillations is uncertain by a multiplicative factor that is almost impossible to determine, this multiplicative factor is likely very similar for all eight channels. Therefore, we believe the relative amplitudes used in our analysis here are largely unaffected by recalibration uncertainties.

For other time periods during the 2020 event, the lack of response in channels adjoining the 3.11 kHz channel does not allow the accuracy obtained above, and we are left with error bars of about ±15% following arguments similar to those used by Gurnett & Kurth (2019) in their Supplementary Information. While we cannot accurately determine the frequency of the 2020 event for most of its duration, it is possible that the lack of a response in either of the adjoining channels, other than during the short interval on day 178, is simply due to a decrease in the amplitude of the emission, and not necessarily due to a change in frequency. We also note that Voyager 1 high spectral resolution observations reveal these as narrowband emissions that have limited spectral variation during an event. The 2014 event described by Gurnett et al. (2015) varies in frequency by no more than about 400 Hz, but this event lasts for the better part of a year.

3. Discussion and Conclusions

We now overlay the new density measurement from Voyager 2 at 124.2 au on Figure 5 of Gurnett & Kurth
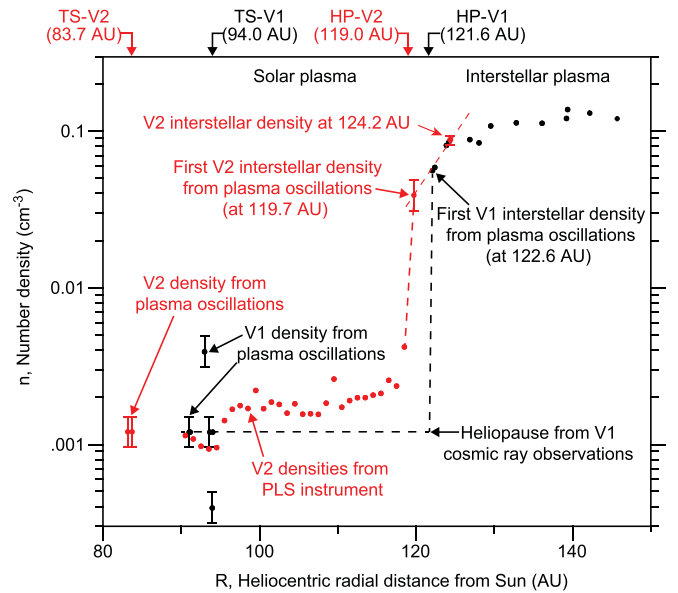

Figure 4. Density inferred from the new Voyager 2 electron plasma oscillation event is superposed on Figure 5 of Gurnett & Kurth (2019). The Voyager 2 density is very similar to that measured by Voyager 1 at the same heliocentric distance. The slope (simply aligned with the two Voyager 2 densities) is very similar to the gradient measured by Voyager 1 with much higher spectral (hence density) resolution in the same post-heliopause region of the local interstellar medium. After Gurnett & Kurth (2019).

(2019) using relative response information from day 178 near 21:15. The result is shown in Figure 4. The new Voyager 2 measurement is nearly coincident with Voyager 1 densities at a similar radial distance. While the slope of the Voyager 2 gradient is poorly constrained because of the uncertainty in the frequency of the point at 119.7 au, it is certainly similar to the Voyager 1 gradient over a similar radial distance range just beyond the heliopause. Using the 0.039 cm^{-3} density reported by Gurnett & Kurth (2019) and the 0.087 cm^{-3} at 124.2 au reported here, the gradient expressed as $\Delta n_e/\Delta R$ is 0.011 cm^{-3} au^{-1}. Using the uncertainty of the density at 119.7 au given by Gurnett & Kurth (2019) and the 8% uncertainty of the new value, the slope can range between 0.009 and 0.014 cm^{-3} au^{-1}. Gurnett et al. (2013) reported an increase in n_e from 0.06 to 0.08 cm^{-3} in 1.5 au for a $\Delta n_e/\Delta R$ of 0.013 cm^{-3}/au. It is clear from Voyager 1 densities given in Gurnett & Kurth (2019) that the magnitude of the slope decreases with distance from the heliopause. Hence, the magnitude of the density gradient inferred from the two Voyager 2 events is strikingly similar to that obtained by Voyager 1.

The new density measurement inferred from the frequency of electron plasma oscillations observed by Voyager 2 combined with the 2019 measurement provides evidence of a positive radial gradient in the VLISM just beyond the heliopause along the Voyager 2 trajectory. A similar gradient has been reported (Gurnett et al. 2013, 2015; Gurnett & Kurth 2019) along the Voyager 1 trajectory. Given the 67° difference in heliographic latitude and 43° difference in heliographic longitude between the two Voyagers, the new Voyager 2 observations imply that the density gradient is a large-scale feature of the VLISM, at least in the general direction of the heliospheric nose that is generally situated between the two Voyagers.

The existence of the radial gradient was inferred by Gurnett et al. (1993) from drifting structures in low-frequency radio

emissions observed from as close as about 12 au from the Sun by both Voyagers. They used the time of flight of solar wind transients responsible for intense Forbush decreases at Earth to the onset of radio emissions in the 2–3 kHz range to conclude that the radio source was between 116 and 177 au from the Sun, and hence in the interstellar medium with a plasma frequency in the few kHz range. The idea was that electron plasma oscillations, suggested earlier (Kurth et al. 1984; Macek et al. 1991; Cairns & Gurnett 1992; Cairns et al. 1992) could mode-convert into radio emissions at locations with plasma frequencies of the order of a few kHz. Gurnett et al. (1993) suggested that shocks associated with global merged interaction regions would eventually be transmitted through the heliopause and generate electron plasma oscillations in the foreshock region, similar to shocks in the solar wind or the bow shocks of planets. As these disturbances move through a density gradient, the plasma oscillations, and therefore radio emissions, would occur at increasingly higher frequencies.

As summarized by Gurnett et al. (2013), there are a number of theories that address a radial gradient upstream of the heliopause. For example, Baranov & Malama (1993), using a gas dynamic model of the interaction between the solar wind and VLISM including H atoms and protons, show a pile-up region upstream of the heliopause in the direction of the incoming VLISM flow. Fuselier & Cairns (2013) compared the gradient observed by Voyager 1 to the plasma depletion layer observed upstream of Earth's magnetopause. As the interstellar medium approaches the heliopause, the magnetic field becomes draped over the heliopause and increases in strength. The resulting increase in the ratio of perpendicular to parallel temperatures of the ions and electrons can drive the electromagnetic ion cyclotron instability with the ultimate loss of plasma from the draping region. A good understanding of the origin of this density gradient is not in hand. One plausible way of differentiating between the pile-up model and the plasma depletion model would be to determine whether the gradient flattens to an asymptotic value (depletion layer) or reverses sign with the density decreasing to a somewhat lower value at larger distances. It is not certain whether the Voyagers will be able to operate far enough to distinguish between these two classes of models.

ORCID iDs

W. S. Kurth https://orcid.org/0000-0002-5471-6202
D. A. Gurnett https://orcid.org/0000-0003-2403-0282

References

Baranov, V. B., & Malama, Yu. G. 1993, JGR, 98, 15,157
Burlaga, L. F., Ness, N. F., Berdichevsky, D., et al. 2019, NatAs, 3, 1007
Burlaga, L. F., Ness, N. F., & Stone, E. C. 2013, Sci, 341, 147
Cairns, I. H., & Gurnett, D. A. 1992, JGR, 97, 6235
Cairns, I. H., Kurth, W. S., & Gurnett, D. A. 1992, JGR, 97, 6245
Fuselier, S. A., & Cairns, I. H. 2013, ApJ, 771, 83
Gurnett, D. A., & Kurth, W. S. 2019, NatAs, 3, 1024
Gurnett, D. A., Kurth, W. S., Allendorf, S. C., & Poynter, R. L. 1993, Sci, 262, 199
Gurnett, D. A., Kurth, W. S., Burlaga, L. F., & Ness, N. F. 2013, Sci, 341, 1489
Gurnett, D. A., Kurth, W. S., Stone, E. C., et al. 2015, ApJ, 809, 121
Krimigis, S. M., Decker, R. B., Roelof, E. C., et al. 2019, NatAs, 3, 997
Krimigis, S. M., Decker, R. M., Roelof, E. C., et al. 2013, Sci, 341, 141
Kurth, W. S., Gurnett, D. A., Scarf, F. L., & Poynter, R. L. 1984, Natur, 312, 27
Macek, W. M., Cairns, I. H., Kurth, W. S., & Gurnett, D. A. 1991, JGR, 96, 3801
Pogorelov, N. V., Heerikhuisen, J., Roytershteyn, V., et al. 2017, ApJ, 845, 9
Richardson, J. D., Belcher, J. D., Garcia-Galindo, P., & Burlaga, L. F. 2019, NatAs, 3, 1019
Scarf, F. L., & Gurnett, D. A. 1977, SSRv, 21, 289
Stone, E. C., Cummings, A. C., Heikkila, B. C., & Lal, N. 2019, NatAs, 3, 1013
Stone, E. C., Cummings, A. C., McDonald, F. B., et al. 2013, Sci, 341, 150